

On the mixing strength in the two lowest 0^- states in ^{208}Pb

A. Heusler

*Max-Planck-Institut für Kernphysik, D-69029 Heidelberg, Germany **

G. Graw, R. Hertenberger, F. Riess, and H.-F. Wirth[†]

Department für Physik, Ludwig-Maximilian-Universität München, D-85748 Garching, Germany

R. Krücken

Physik Department E12, Technische Universität München, D-85748 Garching, Germany

P. von Brentano

Institut für Kernphysik, Universität zu Köln, D-50937 Köln, Germany

With a resolution of 3 keV, the two lowest 0^- states in ^{208}Pb are identified by measurements of the reaction $^{207}\text{Pb}(d, p)$ with the München Q3D magnetic spectrograph in a region where the average level spacing is 6 keV. Precise relative spectroscopic factors are determined. Matrix elements of the residual interaction among one-particle one-hole configurations in a two-level scheme are derived for the two lowest 0^- states in ^{208}Pb . The off-diagonal mixing strength is determined as 105 ± 10 (*experimental*) ± 40 (*systematic*) keV. Measurements of the reaction $^{208}\text{Pb}(p, p')$ via isobaric analog resonances in ^{209}Bi support the structure information obtained.

PACS numbers: 21.10.Jx, 27.80.-w.

I. INTRODUCTION

The nucleus ^{208}Pb offers the singular chance to study a two-level scheme in the space of shell model configurations. Below $E_x = 6.1$ MeV, only two 0^- states among about 120 one-particle one-hole configurations are expected from shell model calculations [1, 2]. They are identified [3] but their structure is not known in detail. With the average residual interaction known from experiment [4, 5] they are predicted to consist essentially of the two lowest configurations $s_{1/2}p_{1/2}$ and $d_{5/2}f_{5/2}$, since the next particle-hole configuration is ten times more distant than an average matrix element of the residual interaction among one-particle one-hole configurations (m.e.).

We took spectra of the reaction $^{207}\text{Pb}(d, p)$ at a resolution of 3 keV [6] up to $E_x = 8$ MeV and identified the two 0^- states in the region $E_x = 5.2 - 5.7$ MeV where the mean level distance is 6 keV.

Most of the low-lying states in ^{208}Pb are considered as excited states created by the coupling of exactly one particle and one hole to the ground state. We postulate that each particle-hole state is completely described as a mixture of a few particle-hole configurations. The ground state of ^{207}Pb is assumed to be a pure $p_{1/2}$ neutron hole state in relation to the ground state of ^{208}Pb . In the $^{207}\text{Pb}(d, p)$ reaction, the particle-hole states in ^{208}Pb with spin 0^- are populated by $L = 0$ transfer only, whereas the 1^- states are populated by both $L = 0$ and $L = 2$ transfer.

For two spin 0^- and nine 1^- states below $E_x = 6.5$ MeV, relative spectroscopic factors are measured. Using the method of Ref. [4] and assuming the two lowest configurations to be almost completely contained in the two lowest 0^- states, matrix elements of the residual interaction between the 0^- configurations $s_{1/2}p_{1/2}$ and $d_{5/2}f_{5/2}$ are deduced.

Results of the inelastic proton scattering on ^{208}Pb via isobaric analog resonances (IAR) in ^{209}Bi populating the two 0^- states and some 1^- states [6, 7] are discussed.

II. EXPERIMENTAL DATA

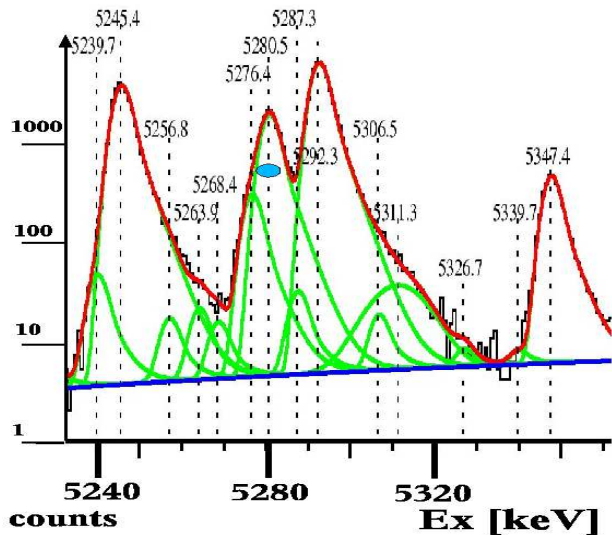
A. Experiments with the Q3D magnetic spectrograph

Using the Q3D magnetic spectrograph of the tandem accelerator of the Maier-Leibnitz laboratory at München, experiments of the reactions $^{207}\text{Pb}(d, p)$ and $^{208}\text{Pb}(p, p')$ via isobaric analog resonances in ^{209}Bi (IAR-pp') are performed. They are described in detail in Ref. [6]. The resolution of about 3 keV, the low background (up to 1:5000) and reliable identification of contamination lines from light nuclei (by the kinematic broadening proportional to different slit openings), and a sophisticated fit of the spectra by the computer code GASPAN [8], allow to resolve nearby levels and to detect weakly excited states. Here we refer to data obtained from the $^{207}\text{Pb}(d, p)$ experiment in the region $E_x = 5.2 - 5.7$ MeV. Compared to earlier work with a resolution of 18 keV from the Heidelberg multi-gap magnetic spectrograph [9] and following work [3, 10, 11, 12], the resolution has been improved and the background lowered.

*correspondance to: A.Heusler@mpi-hd.mpg.de

[†]now at Technische Universität München, D-85748 Garching, Germany

FIG. 1: (online: color) $^{207}\text{Pb}(d, p)$ spectrum taken at $\Theta = 30^\circ$ for $E_x = 5.23 - 5.36$ MeV. The $5280\ 0^-$ state (marked \bullet) is resolved from the two neighbors in 4-7 keV distance. It is displayed on a logarithmic scale since the background is 1/2000 of the maximum peak, but many levels with 1% of the maximum are clearly resolved. The drawn curves show the fit by the computer code GASPAN [8], where the energies are taken from Table I and only the centroid of all energies together and the peak heights are varied. The widths and tails are interpolated from a table generated by inspection of several strong, rather isolated peaks in the whole spectrum covering about 1.2 MeV. A weak contamination line from ^{23}Na is identified near $E_x = 5.31$ MeV.

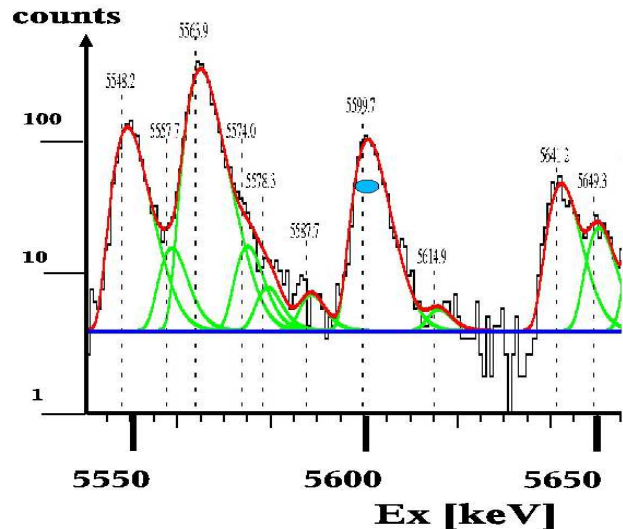


The mean level spacing is about 6 keV in the regions near the two 0^- states. Peaks are identified by comparison to the known data [3, 11, 12, 13, 14, 15], see Table I. A comparison to the preliminary analysis of the $^{208}\text{Pb}(p, p')$ data on seven IAR in ^{209}Bi with similar resolution [6] allows to verify the identifications.

Figs. 1 and 2 show two extracts of $^{207}\text{Pb}(d, p)$ spectra, each covering 1.2 MeV totally. Whereas the neighbors of the $5599\ 0^-$ state are 12-15 keV away, the $5280\ 0^-$ state is surrounded by two levels in 4-7 keV distance. At scattering angles of $\Theta = 20^\circ - 30^\circ$, the 5276 and the 5287 state are excited with cross sections of 1-20% of the 5280 state.

Peaks from light contaminations (^{12}C , ^{14}N , ^{16}O , ^{23}Na and more) are identified in the whole spectra by the kinematic shift in a series of spectra taken at scattering angles $\Theta = 20^\circ - 30^\circ$ and the kinematic broadening for different openings of the entrance slit to the Q3D magnetic spectrograph, see Ref. [6]. In the region of $E_x = 5.5 - 5.7$ MeV, contamination lines from ^{14}N with cross sections of a few $\mu\text{b}/\text{sr}$ are detected at scattering angles $\Theta = 20^\circ$ and 30° .

FIG. 2: (online: color) $^{207}\text{Pb}(d, p)$ spectrum taken at $\Theta = 25^\circ$ for $E_x = 5.54 - 5.65$ MeV. The $5599\ 0^-$ state (marked \bullet) is well isolated. For other details see Fig. 1.



B. Extraction of relative spectroscopic factors

By use of the GASPAN code [8] with the option of fixed energy distances, and the excitation energies from Table I, the cross sections are precisely determined. Figs. 1 and 2 shows spectra for the regions around the $5280\ 0^-$ and the $5599\ 0^-$ levels. Fig. 3 shows the angular distributions for the $5280\ 0^-$, $5292\ 1^-$ and $5599\ 0^-$ levels. For scattering angles $\Theta = 20^\circ - 30^\circ$, the cross sections differ by a constant factor (0.32 and 0.05 for the two 0^- states in relation to $5292\ 1^-$ state) within the errors. For $\Theta = 20^\circ - 30^\circ$, DWBA calculations yield the steep slope observed for $L = 0$ in contrast to a rather flat angular distribution for $L = 2$ [11, 12].

In view of the weak cross sections at $\Theta = 20^\circ$, especially for the $5599\ 0^-$ state, we determine relative spectroscopic factors by first calculating a mean angular distribution of the three states,

$$\widetilde{\frac{d\sigma}{d\Omega}}(\Theta) = \sum_{E_x} \left\{ \frac{d\sigma}{d\Omega}(E_x, \Theta) / \sum_{\theta} \frac{d\sigma}{d\Omega}(E_x, \Theta) \right\}. \quad (1)$$

The energy dependence of the cross section is neglected because of the small energy range. In a least squares fit we then obtain the mean cross section

$$\left\langle \frac{d\sigma}{d\Omega}(E_x) \right\rangle = \sum_{\theta} \left\{ \frac{d\sigma}{d\Omega}(E_x, \Theta) / \widetilde{\frac{d\sigma}{d\Omega}}(\Theta) \right\} \quad (2)$$

as a measure of the relative spectroscopic factors. In Table II we adjust the mean values to the cross section of the 5292 state at the scattering angle $\Theta = 25^\circ$.

C. Determination of mixing amplitudes

The lowest negative parity states in ^{208}Pb are assumed to be well described by the shell model as particle-hole states in relation to the ground state of ^{208}Pb . Especially, the two lowest 0^- states $|E_x, I^\pi\rangle$ are assumed to consist of the configurations $|s_{1/2}p_{1/2}\rangle$ and $|d_{5/2}f_{5/2}\rangle$ with admixtures of higher configurations $|C_q\rangle$,

$$\begin{aligned} |5280, 0^-\rangle &= t_{11} |s_{1/2}p_{1/2}\rangle + t_{12} |d_{5/2}f_{5/2}\rangle + \\ &\quad \sum_q t_{1q} |C_q\rangle, \\ |5599, 0^-\rangle &= t_{21} |s_{1/2}p_{1/2}\rangle + t_{22} |d_{5/2}f_{5/2}\rangle + \\ &\quad \sum_q t_{2q} |C_q\rangle. \end{aligned} \quad (3)$$

The $^{207}\text{Pb}(d, p)$ reaction populates the $s_{1/2}p_{1/2}$ component only.

In contrast to spin 0^- , for spin 1^- the shell model predicts eight states below $E_x = 6.5$ MeV. Two configurations, $s_{1/2}p_{1/2}$ and $d_{3/2}p_{1/2}$, of the identified 1^- states (Table II) are excited by the $^{207}\text{Pb}(d, p)$ reaction. Hence the n 1^- states are described by

$$|n, 1^-\rangle = t_{1n1} |s_{1/2}p_{1/2}\rangle + t_{1n3} |d_{3/2}p_{1/2}\rangle + \sum_q t_{1nq} |C_q\rangle. \quad (4)$$

We want to determine the matrix elements of the residual interaction between the two lowest 0^- configurations in ^{208}Pb . In the truncated two-level configuration space of one-particle one-hole configurations, the matrix t is only approximately unitary,

$$tt^\dagger = \begin{pmatrix} 1 - d_{11} & d_{12} \\ d_{21} & 1 - d_{22} \end{pmatrix} \approx \begin{pmatrix} 1 & 0 \\ 0 & 1 \end{pmatrix}. \quad (5)$$

We postulate the deviation from unitarity to be small,

$$d = \begin{pmatrix} d_{11} & d_{12} \\ d_{21} & d_{22} \end{pmatrix} \approx 0. \quad (6)$$

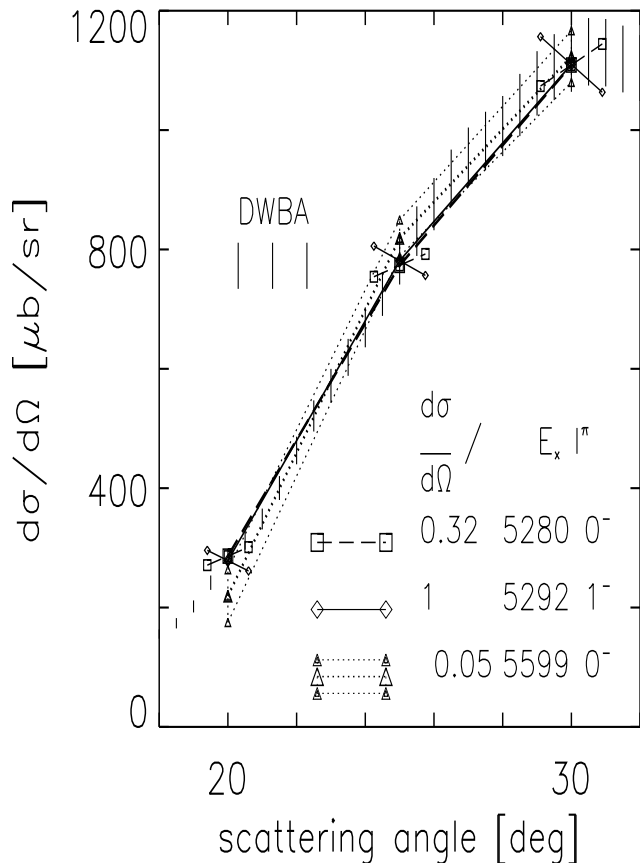
Each element of the deviation matrix contains only products of the amplitudes t_{1q}, t_{2q} of higher configurations assumed to be weak [Eq. (3)] and the amplitudes t_{q1}, t_{q2} of the configurations $s_{1/2}p_{1/2}, d_{5/2}f_{5/2}$ in higher excited states assumed to be weak, too.

According to the shell model without residual interaction, the two configurations $s_{1/2}p_{1/2}$ and $d_{5/2}f_{5/2}$ have the lowest excitation energies for the 1^- states, too. For the 1^- states a similar deviation matrix can be defined with elements d_{1n1}, d_{1n2} , $n = 1, 9$ referring to these two configurations.

An essential assumption is the proportionality of the sum of the strengths of the configuration $s_{1/2}p_{1/2}$ in all states for the spins $I^\pi = 0^-, 1^-$ to the spin factor $(2I+1)$,

$$\sum_n t_{1n1}^2 = 3(t_{11}^2 + t_{21}^2 + d_{11}). \quad (7)$$

FIG. 3: Angular distributions of $^{207}\text{Pb}(d, p)$ for the 5280 0^- , 5292 1^- , 5599 0^- states. At $\Theta = 20^\circ, 25^\circ, 30^\circ$ and for each state, the mean cross section from six runs evaluated with different methods of the background subtraction [6] is shown. The cross section for the two 0^- states are reduced by the given factors. The dashed curve shows the DWBA calculation fitting the data of Refs. [11, 12] for the 5292 1^- state with $L = 0$. For $L = 2$ the DWBA curve and the data for the two levels (5924 2^- , 5947 1^- [3]) bearing the main strength of the $d_{3/2}p_{1/2}$ configuration vary by less than 10% in between $\Theta = 20^\circ - 30^\circ$.



We then use the observation that the configurations $s_{1/2}p_{1/2}$ and $d_{3/2}p_{1/2}$ produce angular distributions which are easily distinguished, to derive upper and lower limits of the complete $s_{1/2}p_{1/2}$ strength $\sum_n t_{1n1}^2$ in the 1^- states and thus derive an upper limit for the deviation matrix $|d|$ by use of Eq. 7.

Since the reaction $^{207}\text{Pb}(d, p)$ excites only the $s_{1/2}p_{1/2}$ component of the 0^- states [Eq. (3)], the ratio of the measured mean cross sections (Table II)

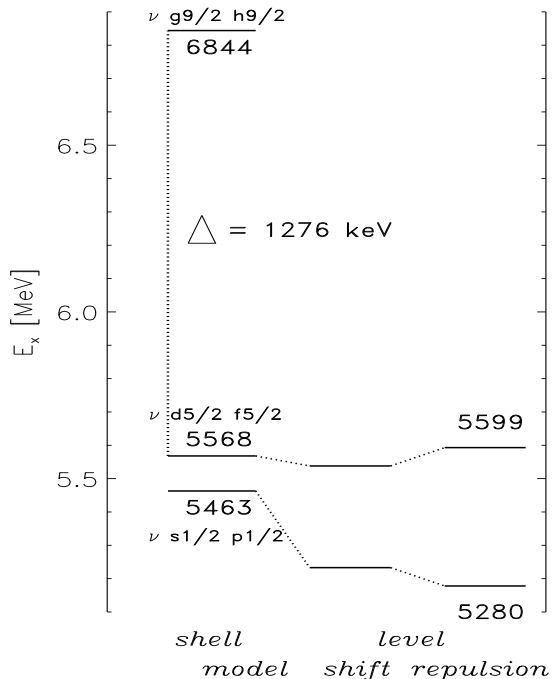
$$t_{21}^2/t_{11}^2 = \left\langle \frac{d\sigma}{d\Omega}(5599) \right\rangle / \left\langle \frac{d\sigma}{d\Omega}(5280) \right\rangle \quad (8)$$

is used to derive the amplitudes $t_{11}, t_{12}, t_{21}, t_{22}$ as

$$\begin{aligned} |t_{11}| &= |t_{22}| = 0.928 \pm 0.012, \\ |t_{12}| &= |t_{21}| = 0.37 \pm 0.04. \end{aligned} \quad (9)$$

Here the deviation matrix d [Eq. (6)] is assumed to vanish.

FIG. 4: The two lowest 0^- configurations in ^{208}Pb are separated from the next higher configurations by a large gap Δ allowing to discuss the simple case of a two-level configuration mixing in the $|5280 0^- \rangle$ and $|5599 0^- \rangle$ states. The residual interaction is decomposed into the m.e. v_{11} and v_{22} describing the shift of the two levels, and the m.e. $v_{12} = v_{21}$ describing the level repulsion.



D. Completeness of the strength in the truncated configuration space

Higher 0^- states are not known, but they should have energies above $E_x \approx 6.8$ MeV, see Fig. 4. In contrast, nine 1^- states are known as predicted by the shell model.

The cross sections $\langle \frac{d\sigma}{d\Omega}(E_x) \rangle$ (Table II) for the two 0^- states and all 1^- states up to $E_x = 6.5$ MeV are consistent with the data of Refs. [11, 12] within the errors. The ratios agree also with the population strengths of Ref. [3] but they are more precise.

The reaction $^{207}\text{Pb}(d, p)$ excites the two configurations $s_{1/2}p_{1/2}$ and $d_{3/2}p_{1/2}$ in all 1^- states, but only the configuration $s_{1/2}p_{1/2}$ in the 0^- states. The two lowest 0^- states contain almost the complete $s_{1/2}p_{1/2}$ 0^- strength by comparison to DWBA calculations [11, 12]. Because higher configurations admix little due to the gap Δ between the second and third 0^- configurations, $d_{5/2}f_{5/2}$ and $g_{9/2}h_{9/2}$, being larger than ten times the mean m.e., the deviation matrix d almost vanishes. By comparing

the detected strength of the 0^- and 1^- $s_{1/2}p_{1/2}$ configurations, we deduce an upper limit for $|d|$.

The 5292 1^- state contains less than 90% of the $s_{1/2}p_{1/2}$ strength, since the ratio of its cross section to the sum of the two 0^- states is less than the ratio 3:1 expected from the spin factor $(2I+1)$ [Eq. (7)]. Other 1^- states contain the remaining $s_{1/2}p_{1/2}$ strength, but the 5292 1^- state contains also some of the $d_{3/2}p_{1/2}$ strength (besides other configurations not detected by $^{207}\text{Pb}(d, p)$ but by IAR-pp'). The missing $s_{1/2}p_{1/2}$ strength is contained in the other eight 1^- states.

(a) All 1^- states except for the 5292 1^- state listed in Table II have rather flat angular distributions for $\Theta = 20^\circ - 30^\circ$. For the states considered, the dependence of the cross section on the energy E_x for states with the same configuration mixture is negligible [11, 12]. (b) For the 5924 2^- and 5947 1^- states, the angular distribution for $\Theta = 20^\circ - 30^\circ$ is flat (similarly as for states with $d_{5/2}p_{1/2}$ strength) in contrast to the steep rise for the $s_{1/2}p_{1/2}$ configuration [11, 12]. The 5924 2^- and 5947 1^- states contain most of the $d_{3/2}p_{1/2}$ strength [11, 12] and the spin assignments are firm [3]. (c) In the 5947 state, the comparison of the shape of the angular distribution to the 5924 2^- state allows to deduce an upper limit for the $s_{1/2}p_{1/2}$ strength of about 8% or a ratio $r_{2:0} = t_{1n3}^2/t_{1n1}^2 > 12$ [Eq. (4)]. (d) The deviation of the slope of the cross section for the 5292 1^- state in comparison to the two 0^- states implies up to 10% $d_{3/2}p_{1/2}$ admixture (Fig. 3). (e) For the other 1^- states besides the 5292 and 5947 states, from the comparison of the shape of the angular distribution to the 5292 1^- and 5924 2^- states the ratio $r_{2:0}$ is derived, see Table II.

Summing up thus derived upper limits of $s_{1/2}p_{1/2}$ admixtures t_{1n1}^2 to all other 1^- states, we derive a lower limit 80% of the $s_{1/2}p_{1/2}$ configuration in the 5292 1^- state.

Together with the upper limit of 90% derived before, from Eq. 7 we conclude the sum of the $s_{1/2}p_{1/2}$ strength in the 5280 0^- and 5599 0^- states to be complete within better than 97%. This yields an upper limit for the deviation matrix [Eq. (6)],

$$\begin{aligned} d_{11} &\approx d_{22} < 0.03, \\ |d_{12}| &\approx |d_{21}| < 0.02. \end{aligned} \quad (10)$$

E. Excitation energies

From the known single particle and single hole states in the lead region [10], the lowest one-particle one-hole configurations in ^{208}Pb with spin 0^- are predicted as $\nu s_{1/2}p_{1/2}$, $\nu d_{5/2}f_{5/2}$, $\nu g_{9/2}h_{9/2}$, $\nu d_{3/2}p_{3/2}$, $\pi p_{3/2}d_{3/2}$ (the lowest proton particle-hole configuration) at $E_x = 5463, 5568, 6844, 6866, 7383$ keV, respectively, see Fig. 4. The gap Δ described by Ref. [4] between the two lowest configurations $s_{1/2}p_{1/2}$ and $d_{5/2}f_{5/2}$ and the next configurations is 1276 keV. Since it is more than ten times higher

than the mean m.e. the mixing of the two lowest 0^- configurations in ^{208}Pb represents an excellent example of a two-level scheme.

The energies of the shell model configurations are derived from the single particle and single hole states in the

four neighboring nuclei [10], $e^0 = \begin{pmatrix} 5463 & 0 \\ 0 & 5568 \end{pmatrix}$ keV. The experimental data yield the excitation energies of the two states, $E = \begin{pmatrix} 5280 & 0 \\ 0 & 5599 \end{pmatrix}$ keV.

TABLE I: Levels near the 5280 0^- and 5599 0^- states in ^{208}Pb (marked \bullet). Within 1-2 keV, the energy label corresponds to the energies from Refs. [3, 11, 12, 13, 14, 15] or this work. The values from Refs. [11, 12] refer to the reaction $^{208}\text{Pb}(p, p')$ at $E_p = 22$ MeV. Spin and parity I^π from Refs. [3, 6, 13, 14, 15] are shown.

energy label	E_x keV <i>this work</i>	E_x keV Ref. [3]	E_x keV Refs. [13, 14]	E_x keV Refs. [11, 12]	I^π	Ref.
region near 5280 0^- and 5292 1^-						
5239	5239.5 ± 0.8	5239.35 ± 0.36			4^-	[6]
5241		5241		5240.8 ± 1.5	0^+	[15]
5245	5245.4 ± 0.3	5245.28 ± 0.06	5245.2 ± 0.1	5244.6 ± 1.0	3^-	[3]
5254	5254.2 ± 0.8	5254.16 ± 0.15				
5261	5261.2 ± 0.8					
5266	5266.6 ± 0.9					
5276	5276.3 ± 0.4			5277.1 ± 1.5	4^-	[6]
\bullet 5280	5280.5 ± 0.1	5280.32 ± 0.08	5280.5 ± 0.1	5281.3 ± 1.5	0^-	[3]
5287	5287.8 ± 1.9			5287.2 ± 1.5		
5292	5292.2 ± 0.1	5292.00 ± 0.20	5292.1 ± 0.1	5292.6 ± 1.5	1^-	[3]
5307	5307.6 ± 1.5					
5316	5313.0 ± 1.0	5317.00 ± 0.20			(3^+)	[3]
5317	5316.9 ± 1.5	5317.30 ± 0.06		5317.7 ± 0.6		
5326				5326.9 ± 0.6		
5339	5340.0 ± 0.9	5339.46 ± 0.16		5340.1 ± 1.5	8^+	[3]
5347	5347.4 ± 0.2	5347.15 ± 0.25		5348.4 ± 0.6	3^-	[3]
region near 5599 0^-						
5548	5548.5 ± 0.4	5548.08 ± 0.20	5548.2 ± 0.1	5547.5 ± 1.5	2^-	[3]
5557	5557.2 ± 1.0			5554.0 ± 2.0		
5563	5563.9 ± 0.3	5563.58 ± 0.14	5563.6 ± 0.1	5564.7 ± 0.6	$3^-, 4^-$	[3]
5566		5566.00 ± 0.60			4^-	[3]
5572	5572.0 ± 0.8					
5577	5579.0 ± 0.9			5576.6 ± 1.5		
5587	5587.4 ± 1.0			5587.7 ± 0.5		
\bullet 5599	5599.8 ± 0.5	5599.40 ± 0.08	5601.7 ± 0.1	5599.6 ± 0.4	0^-	[3]
5614	5614.4 ± 1.7			5615.4 ± 0.4		
5641	5640.7 ± 0.6	5641.10 ± 0.50	5641.4 ± 0.5	5639.9 ± 1.5	$(1^-, 2^+)$	[13, 14]
5643				5643.1 ± 1.5		
5649	5648.7 ± 0.5	5649.70 ± 0.28		5649.8 ± 0.9	(5^-)	

III. RESULTS AND DISCUSSION

A. Determination of matrix elements of the residual interaction

The matrix elements of the residual interaction between the two lowest 0^- configurations are derived in the truncated space of the first two configurations by the

method described in Ref. [4],

$$v = tEt^\dagger - \frac{1}{2}(tt^\dagger e^0 + e^0 tt^\dagger) + r, \quad (11)$$

where r is the residual matrix describing the influence of the higher configurations $|C_q\rangle$ in the space separated from the two lowest configurations by the gap Δ (Fig. 4).

Explicitly we have

$$\begin{aligned}
v_{11} &= t_{11}^2 E_{11} + t_{12}^2 E_{22} - (t_{11}^2 + t_{12}^2) e_{11}^0 + r_{11}, \\
v_{22} &= t_{21}^2 E_{11} + t_{22}^2 E_{22} - (t_{21}^2 + t_{22}^2) e_{22}^0 + r_{22}, \\
v_{12} &= t_{11} t_{21} E_{11} + t_{12} t_{22} E_{22} - \\
&\quad \frac{1}{2} (t_{11} t_{21} + t_{12} t_{22}) (e_{11}^0 + e_{22}^0) + r_{12}, \\
v_{21} &= t_{21} t_{11} E_{11} + t_{22} t_{12} E_{22} - \\
&\quad \frac{1}{2} (t_{21} t_{11} + t_{22} t_{12}) (e_{11}^0 + e_{22}^0) + r_{21}. \quad (12)
\end{aligned}$$

Using Eqs. (9, 10, 12) we obtain the m.e.

$$\begin{aligned}
v_{11} &= -140 \pm 10 \text{ (exp.)} \pm 40 \text{ (syst.) keV}, \\
v_{22} &= -5 \pm 10 \text{ (exp.)} \pm 40 \text{ (syst.) keV}, \\
v_{12} = v_{21} &= \pm(105 \pm 10) \text{ (exp.)} \pm 40 \text{ (syst.) keV}. \quad (13)
\end{aligned}$$

The sign of the off-diagonal terms v_{12}, v_{21} cannot be determined from our data. The diagonal terms v_{11}, v_{22} describe the level shift, the off-diagonal terms v_{12}, v_{21} the level repulsion, see Fig. 4.

The m.e. (especially the off-diagonal m.e.) agree with the mean m.e. of about 100 keV obtained from the analysis of the lowest 20 particle-hole configurations in ^{208}Pb , see [4, 5]. The values v are compatible with theoretical calculations [1, 2], but more precise.

The systematic error is well estimated for the diagonal m.e. [4] by use of the deviation matrix d [Eq. (10)]. The systematic error for the off-diagonal m.e. is estimated from the residual matrix element

$$r_{12} = \sum_q (t_{11} E_{11} t_{q1} + t_{1q} E_{qq} t_{11}). \quad (14)$$

From Eqs. (5, 10) we derive contributions from higher states and higher configurations to be small, $|t_{1q}| < 0.14, |t_{q1}| < 0.14$. Shell model calculations support the assumption of statistically distributed signs for the amplitudes t_{1q}, t_{q1} . So, a systematic error of the off-diagonal m.e. of about 40 keV may be assumed.

B. Data from IAR-pp'

A preliminary analysis of the IAR-pp' data [6] is consistent with the spin assignments given in Table II. Especially the $5292\ 1^-, 5924\ 2^-, 5947\ 1^-$ states are selectively excited by the $s_{1/2}, d_{3/2}, d_{3/2}$ IAR, respectively.

In early IAR-pp' experiments [7] excitation function were measured for several multiplets with a resolution of 26 keV. The energies given by Ref. [7] derive from the calibration of IAR-pp' spectra taken with the Enge split-pole magnetic spectrograph [16]. They are about 0.13% too low [6].

Measurements of the excitation function for the unresolved $5280\ 0^-, 5292\ 1^-$ doublet ("5.284 MeV") show a strong excitation by the $s_{1/2}$ IAR. A weak excitation by the $d_{5/2}$ IAR is explained by the $d_{5/2}f_{5/2}$ component in the $5280\ 0^-$ state [Eqs. (3, 9)] and $d_{5/2}f_{5/2}, d_{5/2}p_{3/2}$ components in the $5292\ 1^-$ state [Eq.4].

Similarly the resolved $5924\ 2^-, 5947\ 1^-$ doublet ("5.914 + 5.936 MeV") is dominantly excited by the $d_{3/2}$ IAR proving the presence of about equal $d_{3/2}p_{1/2}$ components in both states in agreement with the results from $^{207}\text{Pb}(d, p)$. Whereas the 5924 state clearly resonates on the $s_{1/2}$ IAR (which is explained by weak $s_{1/2}f_{5/2}$ and $s_{1/2}p_{3/2}$ components), the decay curve of 5947 state near the $s_{1/2}$ IAR is smooth.

The $d_{5/2}$ and $s_{1/2}$ IAR are not well isolated, $E^{res} = 16.496, 16.965\ \text{MeV}$ and $E^{tot} = 45 \pm 5, 45 \pm 8$, respectively [6, 7]. Assuming isolated IAR and using the amplitudes of Eq. (13), a calculation of the cross sections for the $5280\ 0^-$ and $5599\ 0^-$ states on the $d_{5/2}$ and $s_{1/2}$ IAR (using the IAR parameters of Ref. [6]) roughly agrees with the measured data. An essay following Ref. [17] to describe the angular distributions by interfering IAR did not yield conclusive results essentially because of missing data at scattering angles $\Theta < 40^\circ$.

IV. SUMMARY

Up to $E_x = 6.1\ \text{MeV}$, the shell model predicts about 120 one-particle one-hole states in ^{208}Pb but only two states with spin 0^- . From a measurement of the reaction $^{207}\text{Pb}(d, p)$ at a resolution of 3 keV, we identify the two known states with spin 0^- among about 150 states in a region where the mean level spacing is 6 keV. Spectroscopic information for the two 0^- states is used to determine their structure.

Matrix elements of the residual interaction for the unique case of a two-level mixing between the two lowest 0^- configurations in ^{208}Pb are derived with higher precision than current shell model calculations. Spectroscopic information for the nine lowest 1^- states is used to quantify the systematic uncertainty.

Additional data from inelastic proton scattering via IAR in ^{209}Bi support the structure information obtained.

Acknowledgments

This work has been supported by MLL, DFG C4-Gr894/2-3, and DFG Br799/12-1.

TABLE II: Up to $E_x = 6.5$ MeV, for the two states with spin 0^- (marked \bullet) and nine states with spin 1^- , the mean cross section $\langle \frac{d\sigma}{d\Omega}(E_x) \rangle$ [see Eq. (2)] adjusted to reproduce the cross section at $\Theta = 25^\circ$ for the 5292 1^- state is shown. Within 1-2 keV, the energy label reflects the energies E_x from Refs. [3, 11, 12, 13, 14] or this work. Spectroscopic factors $S_{(d,p\gamma)}$ [3] and S.F. [11, 12] are given for comparison. The reaction $^{207}\text{Pb}(d, p)$ was measured with the same deuteron energy $E_d = 22.000$ MeV as Refs. [11, 12]. In the states with spin 1^- , the $L = 0$ and $L = 2$ transfer excites the $s_{1/2}p_{1/2}$ and $d_{3/2}p_{1/2}$ configurations, respectively, but in the two 0^- states only the $s_{1/2}p_{1/2}$ component is excited by the $L = 0$ transfer [Eqs. (3), (4)]. From the measured angular distributions, we derive the ratio $r_{2:0}$ of the strength t^2 for the configurations $d_{3/2}p_{1/2}$ ($L = 2$) and $s_{1/2}p_{1/2}$ ($L = 0$). Namely, the angular distribution for $L = 2$ is flat in contrast to the steep slope for $L = 0$. For the same S.F. the relative cross section at $\Theta = 25^\circ$ $\langle \frac{d\sigma}{d\Omega}(E_x) \rangle$ rates as about 1 : 0.5 for $L = 2$ to $L = 0$ [11, 12].

n	Energy label	I^π	$S_{(d,p\gamma)} \times 1000$		L	S.F. $\times 1000$	$r_{2:0}$	$\langle \frac{d\sigma}{d\Omega}(E_x) \rangle \mu\text{b}/\text{sr}$	
			Ref. [3]					Refs. [11, 12]	this work
1	4841	1^-	0	11 ± 4			>0.5	22 ± 5	
\bullet	5280	0^-	0	377 ± 32	0	650	0	250 ± 10	
2	5292	1^-	0	1071 ± 325	0	1550	<0.1	785 ± 30	
3	5512	1^-	0	74 ± 22			>0.8	160 ± 15	
					2	165			
\bullet	5599	0^-	0	60 ± 6	0	103	0	40 ± 5	
4	5641	1^{-1}		4^2			>0.7	22 ± 3	
5	5947	1^-	2	1266 ± 488	2	1390	$>12^3$	1300 ± 80^4	
6	6263	1^-	2	55 ± 23	2	7	>0.6	25 ± 10	
					0	59			
7	6314	1^-	2	88 ± 38	0	113	>0.7	38 ± 12	
8	6360	1^-	2	29 ± 13	2	13	>0.7	9 ± 3	
9	6486	1^{-5}		30^2	2	38	>0.8	30 ± 5	
					0	12			

[1] B. Alex Brown. *Phys. Rev. Lett.*, 85:5300, (2000).

[2] M. Rejmund, M. Schramm, K. H. Maier. *Phys. Rev.*, C59:2520, (1999).

[3] M. Schramm, K. H. Maier, M. Rejmund, L. D. Wood, N. Roy, A. Kuhnert, A. Aprahamian, J. Becker, M. Brinkman, D. J. Decman, E. A. Henry, R. Hoff, D. Man-

att, L. G. Mann, R. A. Meyer, W. Stoeffl, G. L. Struble, T.-F. Wang. *Phys. Rev.*, C56:1320, (1997).

[4] A. Heusler and P. von Brentano. *Ann. Phys. (NY)*, 75:381, (1973).

[5] A. Heusler, G. Graw, R. Hertenberger, F. Riess, H.-F. Wirth, T. Faestermann, R. Krücken, J. Jolie, N. Pietralla, P. von Brentano. <http://arxiv.org/abs/nuclex/0601016>.

[6] A. Heusler, G. Graw, R. Hertenberger, F. Riess, H.-F. Wirth, T. Faestermann, R. Krücken, J. Jolie, D. Mürcher, N. Pietralla, P. von Brentano. *Phys. Rev. C*, 74:03403, (2006).

[7] W. R. Wharton, P. von Brentano, W. K. Dawson, P. Richard. *Phys. Rev.*, 176:1424, (1968).

[8] F. Riess. <http://www.cip.physik.uni-muenchen.de/~riess/>.

[9] P. B. Vold, J. O. Andreassen, J. R. Lien, A. Graue, E. R. Cosman, W. Dünneweber, D. Schmitt, and F. Nusslin. *Nucl. Phys.*, A215:61, (1973).

¹ $I^\pi = (1^-, 2^+)$ from Refs. [13, 14]. The preliminary analysis of our data excludes spin 2^+ .

² Derived from the relative population strength (S_{expt}).

³ By comparison to the 5924 2^- state with $L = 2$ only.

⁴ The error includes the variation of the angular distribution with Θ .

⁵ $I^\pi = 1^-$ from Refs. [13, 14].

- [10] M. J. Martin. *Nucl. Data Sheets*, 47:797, (1986).
- [11] B. D. Valnion, V. Yu. Ponomarev, Y. Eisermann, A. Gollwitzer, R. Hertenberger, A. Metz, P. Schiemenz, and G. Graw. *Phys. Rev.*, C63:024318, (2001).
- [12] B. D. Valnion. PhD thesis, Universität München, (1998). Herbert Utz Verlag, München.
- [13] E. Radermacher, M. Wilhelm, S. Albers, J. Eberth, N. Nicolay, H.-G. Thomas, H. Tiesler, P. von Brentano, R. Schwengner, S. Skoda, G. Winter, and K. H. Maier. *Nucl. Phys.*, A597:408, (1996).
- [14] E. Radermacher, M. Wilhelm, P. von Brentano, R. V. Jolos. *Nucl. Inst.*, 620:151, (1997).
- [15] Minfang Yeh, P. E. Garrett, C. A. McGrath, S. W. Yates, and T. Belgya. *Phys. Rev. Lett.*, 76:1208, (1996).
- [16] C. F. Moore, J. G. Kulleck, P. von Brentano, F. Rickey. *Phys. Rev.*, 164:1559, (1967).
- [17] A. Heusler, M. Endriss, C. F. Moore, E. Grosse, P. von Brentano. *Z. Phys.*, 227:55, (1969).